Reaction $\pi^+p \to \pi^+\pi^0p$ near Threshold and Chiral Symmetry Breaking

D. Počanić, E. Frlež, K. A. Assamagan, J. P. Chen,* K. J. Keeter,† R. M. Marshall, R. C. Minehart, and L. C. Smith
Department of Physics, University of Virginia, Charlottesville, Virginia 22901

G. E. Dodge,‡ S. S. Hanna, and B. H. King§
Department of Physics, Stanford University, Stanford, California 94305

J. N. Knudson
Los Alamos National Laboratory, Los Alamos, New Mexico 87545
(Received 9 June 1993)

We have measured total cross sections for the reaction $\pi^+p \to \pi^+\pi^0p$ at incident pion kinetic energies of 190, 200, 220, 240, and 260 MeV. We use this result to deduce a new value of the chiral symmetry breaking parameter, $\xi = -0.25 \pm 0.10$, in a global constrained fit of the five $\pi\pi N$ near-threshold amplitudes. Consequently, we report new soft pion model values for the s-wave $\pi\pi$ scattering lengths.

PACS numbers: 13.75.Gx, 11.30.Rd

Quantum chromodynamics (QCD) is universally accepted as the theory of strong interactions, largely because of its considerable success in describing processes involving large momentum transfer, i.e., short interaction distances. At intermediate and low energies, however, as the coupling constant becomes large, QCD becomes nonperturbative and practically intractable by available calculational methods. In order to overcome this problem, a broad theoretical effort is under way to develop phenomenological Lagrangian models based solely on the symmetry properties of the full QCD, as suggested by Weinberg [1]. Among the symmetries of the strong interaction, chiral symmetry is of particular significance at low energies, since it is violated only slightly in the SU(2) realization. Indeed, chiral symmetry is essential to the understanding of the lightest hadrons, and it provides the framework for all effective Lagrangian models, e.g., the chiral perturbation theory (ChPT) [2], and recent QCD formulations of the Nambu–Jona-Lasinio model in SU(2) and SU(3) flavor space (for a comprehensive recent review see [3]). A full understanding of the mechanism of chiral symmetry breaking is, therefore, imperative.

The $\pi\pi$ system at zero momentum provides the most sensitive means to study chiral symmetry breaking, since $\pi\pi$ scattering lengths vanish in the chiral limit [4]. Early models of chiral symmetry breaking gave predictions of $a_0^{0,2}(\pi\pi)$, the $I = 0, 2$ s-wave scattering lengths, based mainly on current algebra and PCAC (partial conservation of axial-vector current) [4–6]. Using soft-pion theory, Olsson and Turner [7] parametrized the different predictions in terms of ξ, a single chiral symmetry breaking parameter. More recent calculations of $\pi\pi$ scattering lengths include the work of Jacob and Scadron [8], Gasser and Leutwyler [9] (ChPT), and Ivanov and Troitskaya [10] (model of dominance by quark loop anomalies, QLAD).

Aside from the decay $K^- \to \pi^-\pi^+e^-\overline{\nu}$, all of the information on the $\pi\pi$ interaction has been extracted from studies of the $\pi N \to \pi\pi N$ reactions. After a period without much new data, the past few years have brought about a number of measurements of the $\pi N \to \pi\pi N$ reactions close to threshold [11–13]. Consequently, Burkhardt and Lowe [14] incorporated the existing $\pi\pi N$ data in a comprehensive soft-pion analysis which produced a consistent global solution for the isospin amplitudes, and, hence, a new value for ξ. However, the available data in the $\pi^+\pi^0p$ channel below 300 MeV were scarce and of accuracy too low to constrain the global fit. Moreover, the analysis was complicated by inconsistencies in the published cross sections for the $\pi^+\pi^+n$ channel.

The present work studies the $\pi^+p \to \pi^+\pi^0p$ channel in the region of incident pion kinetic energy from 190 to 260 MeV (the threshold is at 164.8 MeV). Our purpose is twofold: (i) to extract the angle-integrated cross sections needed for a comprehensive soft-pion analysis, and (ii) to measure exclusive cross sections with sufficiently high accuracy and phase-space coverage to allow a model-independent $\pi\pi$ phase shift analysis. In the interest of timeliness, in this paper we present only the integrated cross sections and their soft-pion analysis, leaving the more complex discussion of exclusive cross sections for a later publication.

Our measurements were performed at the Low Energy Pion beamline of the Los Alamos Meson Physics Facility. Pion beams with momentum spread $\Delta p/p = \pm(0.15$–$0.2)\%$ were focused on a specially constructed thin-walled liquid hydrogen target. Beam charge was monitored by means of a sealed ion chamber and a current integrator. Almost all protons were removed from the beam by means of a thin degrader at the beam focal point in the middle of the beamline. For each beam energy a residual proton contamination of (0.2–0.7)% was measured by varying the central momentum of the beamline bending

0031-9007/94/72(8)/1156(4)$06.00

magnets downstream of the degrader. Pion content of the beam was determined by activation of ^{11}C in plastic scintillator disk detectors [15]. Long-term reproducibility of this method was about $\pm$ 2% or better, while the π^+ activation cross sections carry uncertainties of (0.9–4)% [15].

The γ rays from neutral pion decays were detected in the LAMPF π^0 spectrometer [16]. Protons and charged pions were detected in a specially constructed 14-telescope array of plastic scintillator detectors. Each telescope included at least one thin (3 mm) and one thick (25 mm) ΔE counter, and a full absorption counter capable of stopping the pions allowed by the kinematics of our reaction. Six telescopes positioned at $\theta_{lab} \geq 40°$ subtended a larger solid angle than the remaining eight. In order to maintain uniform angular resolution, we arranged the thin and thick ΔE counters on each of the six telescopes into a 4×2 hodoscope. In all, 56 distinct angular bins were covered simultaneously.

The efficiency of the π^0 spectrometer was determined in a series of measurements using the pion charge exchange reaction at $T_\pi^{lab} = 30$ MeV on a CH_2 target, and studying the spectrometer response to penetrating cosmic muons. Individual efficiencies were measured for every detector in the spectrometer, and the entire π^0 spectrometer assembly was simulated with the Monte Carlo code GEANT3 [17]. The overall uncertainty in the efficiency, $\pm$4%, is dominated by the shower tracking efficiency uncertainty (3%). We determined the thickness of our liquid hydrogen target to 3% accuracy by comparing the charge exchange yield at 30 MeV with the yield from a known CH_2 target. We determined the efficiency of the charged particle detectors by detecting elastically scattered π^+ and protons in a separate, prescaled trigger throughout the experiment. This trigger also served as an on-line monitor of the liquid hydrogen target thickness.

We detected and recorded $\pi^0\pi^+$ and $\pi^0 p$ coincident events, as well as the triple coincidences, $\pi^0\pi^+ p$. Detector acceptances, particle kinematics, and background sources for the three categories of events were very different. Thus, the three sets of data had to be analyzed separately, and can be regarded as three essentially independent measurements. In this way, the experiment has a built-in consistency check. Acceptances were calculated using a suitably modified version of the PIANG code [18], and checked independently using GEANT3 [17], with excellent agreement. Measurements were made at $T_\pi = 160$ MeV, below the threshold of π^0 production, to ascertain that the signal vanished for all three event types.

Figure 1 shows the missing mass spectra at 260 MeV for (a) $\pi^0 p$ and (b) $\pi^0\pi^+$ coincident events, after subtraction of accidental and empty-target backgrounds. Both sets of data agree well with the Monte Carlo predicted distributions (shown as histograms), which incorporate

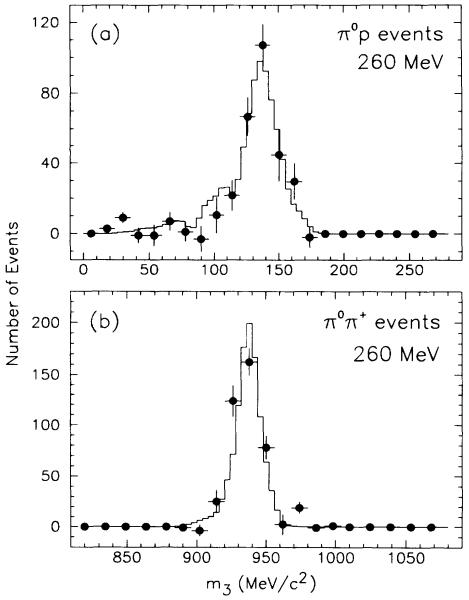

FIG. 1. Measured spectra of the invariant mass of the undetected particle for (a) $\pi^0 p$ and (b) $\pi^0\pi^+$ coincidences at 260 MeV, after subtraction of accidental and target-empty backgrounds (full circles). Histograms shown are the result of a Monte Carlo calculation which incorporates the effects of detector acceptances and resolutions, charged particle detection thresholds, and target size. Results at lower energies are similar.

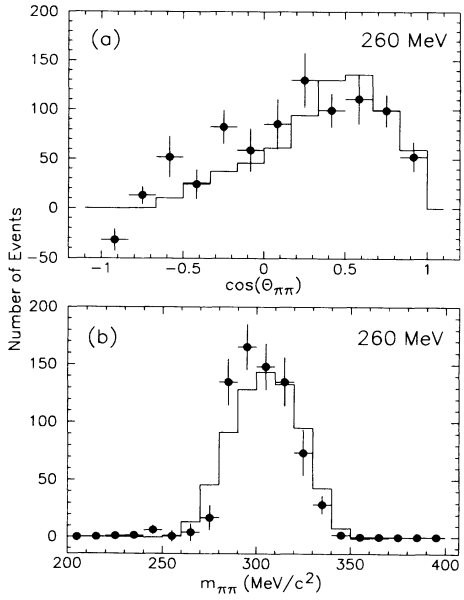

FIG. 2. (a) Distribution of $\cos(\theta_{\pi\pi})$, the dipion polar angle, measured at 260 MeV (full circles), and the results of a Monte Carlo simulation (histogram). (b) Dipion invariant mass distribution measured at 260 MeV (full circles) and simulated (histogram). The Monte Carlo simulation is based on pure s-wave dynamics (phase-space probability distributions), and incorporates the actual detector acceptances and resolutions and the target size.

the effects of instrumental resolution and acceptance, detection thresholds for charged particles, and target size. The FWHM of both distributions is about 30 MeV/c^2. Similar agreement is observed at the four lower energies in our measurement.

In Fig. 2(a) we compare the distribution of $\cos(\theta_{\pi\pi})$, the dipion polar angle, measured at 260 MeV, with a realistic Monte Carlo simulation based on pure s-wave kinematics (phase space), and on our instrumental resolution and acceptance. In the same way, the dipion invariant mass distribution measured at 260 MeV is presented in Fig. 2(b). We observe no significant departure from the phase-space distributions for either quantity; this remains true at lower energies, as well. Hence, the evaluation of angle-integrated cross sections from the recorded yields is straightforward.

Table I lists the total cross sections for π^0 production deduced from the recorded $\pi^0\pi^+$, $\pi^0 p$, and triple coincidences. Cross sections given in the last column of Table I represent appropriately weighted averages of the three measurements (where available), and are our adopted values. Cross section uncertainties quoted in Table I are only statistical. In addition, an overall systematic uncertainty of approximately 9% applies to all data points, and has to be added in quadrature to the statistical uncertainty. This uncertainty is due to six approximately equal contributions, associated with the target thickness, incident π^+ normalization, π^0 absorption, π^0 and charged particle detection efficiencies, and detector acceptances.

The measured total cross sections are plotted against beam energy in Fig. 3(a), which includes all available data in the energy region studied [11,19,20].

Following the method of Olsson and Turner [7], we have extrapolated the moduli of the reaction matrix elements $a(\pi\pi N)$ to zero kinetic energy in the $\pi\pi N$ barycentric system, $T^* = 0$, for all five charge channels, adding our data to the existing database, and imposing the constraints at T^*=0:

$$a(\pi^+\pi^+n)/2 = -\sqrt{2}a(\pi^\pm\pi^0 p) = a(\pi^0\pi^0 n) + a(\pi^+\pi^- n).$$

TABLE I. Total cross sections of the reaction $\pi^+ p \to \pi^+\pi^0 p$ deduced from measurements of $(\pi^0\pi^+)$, $(\pi^0 p)$, and triple coincidences, respectively, as a function of incident pion energy. The incident energy ranges indicated in the first column correspond to the beam momentum spread. Missing entries in the table correspond to measurements with acceptances too small to allow a statistically significant determination of the cross section after background subtraction. The last column lists the appropriately weighted average values. The quoted cross section uncertainties are statistical. There is an additional overall systematic uncertainty of 9% which applies to all data points.

$T_\pi^{\rm lab}$ (MeV)	$\pi^0\pi^+$ σ (μb)	$\pi^0 p$ σ (μb)	$\pi^0\pi^+ p$ σ (μb)	Average σ (μb)
259.5 ± 0.7	26.1 ± 3.7	24.8 ± 5.5	27.0 ± 5.4	26.0 ± 2.7
239.5 ± 0.7	15.5 ± 3.7	14.9 ± 4.5	11.1 ± 6.4	14.6 ± 2.6
219.5 ± 0.6	7.0 ± 2.2	...	6.2 ± 3.4	6.8 ± 1.8
199.5 ± 0.6	2.6 ± 1.3	...	2.9 ± 2.9	2.7 ± 1.2
189.5 ± 0.5	1.5 ± 2.1	...	0 ± 3	1.0 ± 1.7

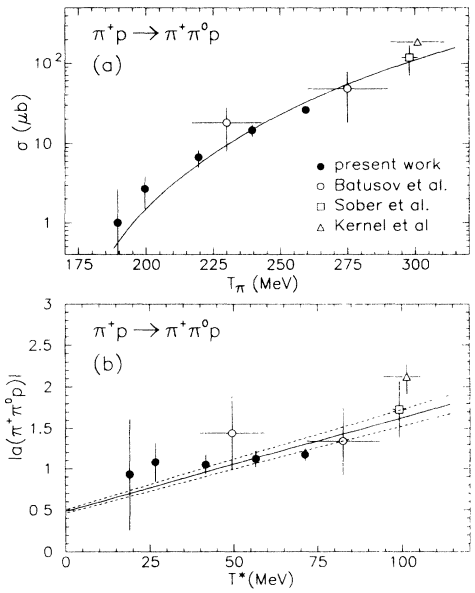

FIG. 3. (a) Total cross sections for the reaction $\pi^+ p \to \pi^+\pi^0 p$ as measured in this work (full circles), and previously published [11,19,20]. Full curve: new global fit of $\pi N \to \pi\pi N$ isospin amplitudes. (b) Absolute values of the $\pi^+\pi^0 p$ matrix element corresponding to the total cross sections shown in (a) as a function of T^*, the total c.m. kinetic energy. Solid and broken lines: global linear fit and the associated uncertainties, respectively.

In our analysis we have used $m_\pi = 137.5$ MeV, $f_\pi = 90.1$ MeV, $M = 938.9$ MeV, and $g_A/g_V = 1.29$, as in Ref. [14], and exact relativistic phase-space factors to extract the matrix element moduli. Like Burkhardt and Lowe [14], we have used linear energy dependence of the amplitudes above threshold. Figure 3(b) shows the constrained fit of the $\pi^+\pi^0 p$ amplitudes (the other four channels display similar agreement). The minimum χ^2 of the global fit is 96 for 93 degrees of freedom [21], resulting in the new value of the chiral symmetry breaking parameter $\xi = -0.25 \pm 0.10$. Our value of ξ differs from that obtained in Ref. [14] (-0.60 ± 0.10). The discrepancy is due primarily to slightly different amplitude constraints above threshold used in the two analyses, and to a lesser extent to differences in the data bases considered. Within the soft-pion model the new value of ξ fixes the $\pi\pi$ s-wave scattering lengths at

$$a_0^0(\pi\pi) = (0.177 \pm 0.006)\, m_\pi^{-1}\ ,$$

$$a_0^2(\pi\pi) = -(0.041 \pm 0.003)\, m_\pi^{-1}\ .$$

These values are to be taken with reservations because they do not reflect any uncertainties inherent in the anal-

ysis method. The Olsson-Turner model has well known limitations and is not based on QCD. ChPT provides a more rigorous framework; however, published direct ChPT calculations of the $\pi N \to \pi\pi N$ amplitudes have been limited to the tree level, and agree poorly with data [22].

In conclusion, our total cross sections are close to those measured in the $\pi^-\pi^0 p$ channel [11], which, from symmetry arguments, is to be expected near threshold. A new global soft-pion fit including our data gives values of the $\pi\pi$ scattering lengths close to the predictions of Weinberg [4] and ChPT [9]. It will be more interesting, however, to extract $a_0^{0,2}(\pi\pi)$ from the now available exclusive data using the approach of Bolokhov *et al.* [23], which is free of dynamical model assumptions, as well as to compare the new data with more realistic ChPT calculations, once they become available.

We thank the staff of LAMPF groups MP-7 and MP-8 for strong technical support, without which our measurements would not have been possible. We are particularly indebted to Bob Garcia who was responsible for the liquid hydrogen target design and construction. We gratefully acknowledge the help of T. Averett, L. Suddarth, M. Lesko, and A. Wall of U. Va. in detector assembly and data taking. Our thanks are due to Julian Noble for many useful discussions and for his support of the experiment from the very beginning. We also thank J. Beringer, A. Bolokhov, and J. Gasser for a number of useful discussions. This work was supported by the U.S. National Science Foundation and Department of Energy.

* Present address: Massachusetts Institute of Technology, Laboratory for Nuclear Science, Cambridge, MA 02139.
† Present address: Saskatchewan Accelerator Laboratory, University of Saskatchewan, Saskatoon, Saskatchewan, Canada S7N 0W0.
‡ Present address: Department of Physics and Astronomy, Vrije Universiteit, de Boelellaan 1081, 1081 HV Amsterdam, The Netherlands.
§ Present address: Institut de Physique Nucléaire, Université Catholique de Louvain, Chemin du Cyclotron 2, B-1348 Louvain-la-Neuve, Belgium.

[1] S. Weinberg, Physica (Amsterdam) **96A**, 327 (1979).
[2] J. Gasser and H. Leutwyler, Ann. Phys. (N.Y.) **158**, 142 (1984); Nucl. Phys. **B250**, 465 (1985).
[3] S. P. Klevansky, Rev. Mod. Phys. **64**, 649 (1992).
[4] S. Weinberg, Phys. Rev. Lett. **17**, 616 (1966); **18**, 188 (1967); Phys. Rev. **166**, 1568 (1968).
[5] J. Schwinger, Phys. Lett. **24B**, 473 (1967).
[6] P. Chang and F. Gürsey, Phys. Rev. **164**, 1752 (1967).
[7] M. G. Olsson and L. Turner, Phys. Rev. Lett. **20**, 1127 (1968); Phys. Rev. **181**, 2141 (1969); L. Turner, Ph.D. thesis, University of Wisconsin, 1969.
[8] R. Jacob and M. D. Scadron, Phys. Rev. D **25**, 3073 (1982).
[9] J. Gasser and H. Leutwyler, Phys. Lett. **125B**, 325 (1983).
[10] A. N. Ivanov and N. I. Troitskaya, Yad. Fiz. **43**, 405 (1986) [Sov. J. Nucl. Phys. **43**, 260 (1986)].
[11] G. Kernel *et al.*, Phys. Lett. B **216**, 244 (1989); **225**, 198 (1989); Z. Phys. C **48**, 201 (1990); in *Particle Production Near Threshold, Nashville, 1990*, edited by H. Nann and E. J. Stephenson (AIP, New York, 1991).
[12] M. E. Sevior *et al.*, Phys. Rev. Lett. **66**, 2569 (1991).
[13] J. Lowe *et al.*, Phys. Rev. C **44**, 956 (1991).
[14] H. Burkhardt and J. Lowe, Phys. Rev. Lett. **67**, 2622 (1991).
[15] B. J. Dropesky *et al.*, Phys. Rev. C **20**, 1844 (1979); G. W. Butler *et al.*, Phys. Rev. C **26**, 1737 (1982).
[16] H. W. Baer *et al.*, Nucl. Instrum. Methods **180**, 445 (1981).
[17] R. Brun *et al.*, GEANT3, publication DD/EE/84-1, CERN, Geneva, 1987.
[18] S. Gilad, Ph.D. thesis, Tel Aviv University, 1979.
[19] Yu. A. Batusov *et al.*, Yad. Fiz. **21**, 308 (1975) [Sov. J. Nucl. Phys. **21**, 162 (1975)].
[20] D. I. Sober *et al.*, Phys. Rev. D **11**, 1017 (1975).
[21] Details of the global amplitude analysis are given in E. Frlež, Ph.D. thesis, University of Virginia, 1993, and in a forthcoming paper.
[22] J. Beringer, πN Newsletter **7**, 33 (1992).
[23] A. A. Bolokhov, V. V. Vereshchagin, and S. G. Sherman, Nucl. Phys. **A530**, 660 (1991).